Nanoscale Res Lett (2010) 5:1279–1283
DOI 10.1007/s11671-010-9637-7

NANO EXPRESS

Formation of PbSe/CdSe Core/Shell Nanocrystals for Stable Near-Infrared High Photoluminescence Emission

Yu Zhang · Quanqin Dai · Xinbi Li · Qingzhou Cui · Zhiyong Gu · Bo Zou · Yiding Wang · William W. Yu

Received: 6 April 2010 / Accepted: 5 May 2010 / Published online: 1 June 2010

Abstract PbSe/CdSe core/shell nanocrystals with quantum yield of 70% were obtained by the "successive ion layer adsorption and reaction" technology in solution. The thickness of the CdSe shell was exactly controlled. A series of spectral red shifts with the CdSe shell growth were observed, which was attributed to the combined effect of the surface polarization and the expansion of carriers' wavefunctions. The stability of PbSe nanocrystals was tremendously improved with CdSe shells.

Keywords PbSe · CdSe · Core–shell · Near infrared · Emission · Nanocrystals

The authors Yu Zhang and Quanqin Dai contributed equally to this work.

Y. Zhang · Q. Dai · Y. Wang (✉) · W. W. Yu (✉)
State Key Laboratory on Integrated Optoelectronics, College of Electronic Science and Engineering, Jilin University, Changchun 130012, China
e-mail: wangyiding47@yahoo.com.cn

W. W. Yu
e-mail: wyu6000@gmail.com

Y. Zhang · X. Li · W. W. Yu
Department of Chemistry and Biochemistry, Worcester Polytechnic Institute, Worcester, MA 01609, USA

Q. Cui · Z. Gu
Department of Chemistry Engineering, University of Massachusetts Lowell, Lowell, MA 01854, USA

B. Zou
State Key Laboratory of Superhard Materials, Jilin University, Changchun 130012, China

Colloidal IV–VI semiconductor nanocrystals (also known as quantum dots, QDs) are of increasing potential applications in telecommunication, photoelectronic device, and biomedical labeling [1, 2], etc. PbSe QDs are important materials because of the strong confinement effect due to their large Bohr radius and the small band gap in near infrared region. Several approaches have been developed to prepare PbSe QDs with uniform size and high quantum yields [3–5]. However, it has been found that PbSe QDs are not stable [6, 7]. PbSe/PbS [8] and PbSe/SiO_2 [9] core/shell structures have been synthesized to stabilize PbSe QDs. But CdSe should be a better shell material due to the higher stability under air condition, the lower lattice mismatch of $\sim$1%, and the little change of the surface chemistry and physics. It is difficult to grow CdSe shells upon PbSe cores using typical cadmium oleate anion precursor because of high reaction temperatures needed. Hollingsworth's group recently developed a method of ion exchange to form PbSe/CdSe core/shell structures in which Cd atoms replaced Pb atoms in the outlayers of large PbSe QDs [10]. However, it may not be easy to control the thickness of the CdSe layers. In this work, we employed the "successive ion layer adsorption and reaction (SILAR)" technology [11] to form air-stable PbSe/CdSe QDs with strong photoluminescence. The quantum yield of PbSe/CdSe QDs was 70%.

Monodisperse colloidal PbSe QDs with high quantum yield were synthesized using literature's method [4]. Two solutions were prepared for CdSe shell growth. A cadmium injection solution (0.04 M) was prepared by heating cadmium cyclohexanebutyrate (0.1804 g) in oleyamine (8.130 g) at 60°C under N_2 flow to obtain a clear colorless solution. A selenium injection solution (0.04 M) was prepared by mixing selenium powder (0.0316 g) in octadecene (7.880 g) at 220°C under N_2 flow until a clear yellow solution was obtained. Both injection solutions were later

used at room temperature. For a typical shell formation, PbSe QDs (4.8 nm in diameter, 1.01×10^{-4} mmol of particles [12]) dispersed in 5 ml of hexanes were loaded into a 25-ml three-neck flask and mixed with 1.500 g of octadecylamine and 5.000 g of octadecene. A mechanical pump was employed at room temperature for 30 min to remove hexanes from the flask. Subsequently, the reaction mixture was heated to 120°C under N_2 flow. Then, the predetermined amounts of the cadmium and selenium solutions were alternatively injected into the three-neck flask drop by drop with syringes using standard air-free procedures. The reaction time for each anion and cation layer was 10 min. The reaction was stopped by the injection of room-temperature toluene. Transmission electron microscope (TEM) was used to characterize PbSe and PbSe/CdSe core/shell QDs as shown in Fig. 1.

Figure 2 shows the evolution of absorption and photoluminescence spectra of the PbSe/CdSe QDs upon the series growth of three monolayers of CdSe shells on the 4.8 nm PbSe cores. The thickness of each shell is 0.35 nm. A consistent red shift of the peak wavelength was observed in both the absorption and PL spectra. The red shifts of the first excitonic absorption peak for three layers were 11, 10, and 11 nm, respectively. The red shift of absorption and PL spectra depends on several factors including (1) the connection between PbSe and CdSe renders the expansion of the carriers' wavefunctions out of the core region with different expansion probabilities resulting in the increase of exciton distance and (2) the surface polarization due to the different dielectric constants of PbSe and CdSe materials.

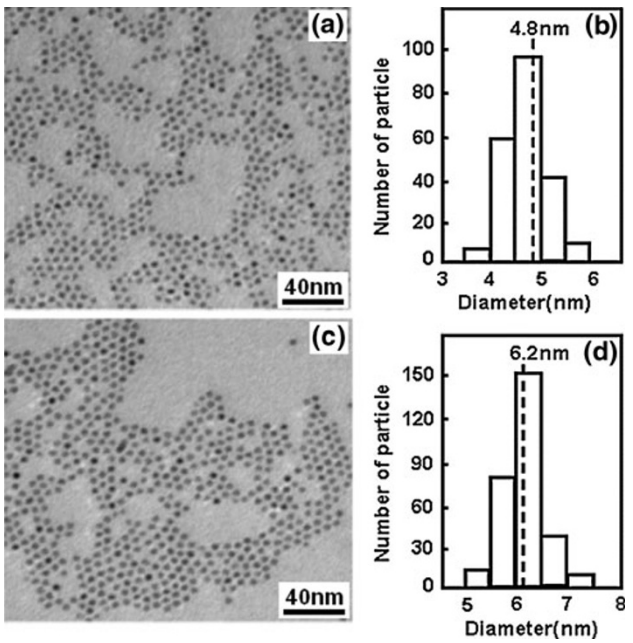

Fig. 1 TEM images and histograms of 4.8 nm PbSe (**a**, **b**) and 6.2 nm PbSe/CdSe (**c**, **d**) QDs. The PbSe and PbSe/CdSe QD samples shown here have narrow size distributions of 8.1% (**b**) and 6.9% (**d**), respectively

The optical gap (E_{gap}) of PbSe QDs is the minimum energy needed to excite an electron from the valence band to the conduction band. The optical gap is given by [13]

$$E_{gap} = (E_e^0 - E_h^0) + (E_e^{conf} + E_h^{conf}) + (E_e^{pol} + E_h^{pol}) - J_{eh}, \quad (1)$$

where E_e^0, E_h^0 are bulk material kinetic energies of the electron and hole, respectively; $E_{gap}^0 = (E_e^0 - E_h^0)$ is band gap of bulk material; E_e^{conf}, E_h^{conf} are the confinement kinetic energies of electron and hole, respectively; E_e^{pol}, E_h^{pol} are the surface-polarization energies of the electron and hole, respectively; and J_{eh} is the direct electron–hole Coulomb attraction. The size of the PbSe QDs (4.8 nm) is much smaller than the Bohr radius (46 nm); therefore, in the strong confinement realm, the energy difference between the electron and hole should be as followed [14]

$$(E_e^{conf} + E_h^{conf}) = \frac{\hbar^2 \pi^2}{2 m_r R^2}, \quad (2)$$

where R is the radius of quantum dot particle; and m_r is the reduced mass of the electron and hole. The energy of Coulomb attraction is given by

$$J_{eh} = \int \psi_e^*(\vec{r}) V_{eh}(\vec{r}) \psi_h(\vec{r}) d\vec{r}, \quad (3)$$

where $\psi_e(\vec{r})$, $\psi_h(\vec{r})$ are the wavefunctions of the electron and hole, respectively; and $V_{eh}(\vec{r})$ is the potential function of the electron and hole. J_{eh} relies on the overlap of wavefuctions' between the electron and hole.

The surface-polarization energies of the electron and hole are

$$E_i^{pol} = \int \left|\psi_i(\vec{r})\right|^2 E(\vec{r}) d\vec{r} \quad i = e, h, \quad (4)$$

where $E(\vec{r})$ is the surface polarization potential

$$E(\vec{r}) = \frac{1}{2} \lim_{\vec{r}' \to \vec{r}} [W_{dot}(\vec{r}, \vec{r}') - W_{bulk}(\vec{r}, \vec{r}')]. \quad (5)$$

where $W_{dot}(\vec{r}, \vec{r}')$ is the screened Coulomb potential of the QD at point $\vec{r}$ due to a point charge located at $\vec{r}'$, and $W_{bulk}(\vec{r}, \vec{r}')$ is the same quantity in the corresponding bulk material system.

PbSe/CdSe core/shell is heterostructured. The energy levels of PbSe and CdSe are shown in Fig. 3. When two semiconductors contact, both electron and hole will induce tunnelling effect and the wavefunctions will diffuse into CdSe shells. The transmission coefficient can be given as [15]

$$t = e^{-\frac{2}{\hbar}\sqrt{2m\Delta E}a} \quad (6)$$

where ΔE is energy barrier at the interface of core/shell structure; m is the effective mass of diffusing particle; a is

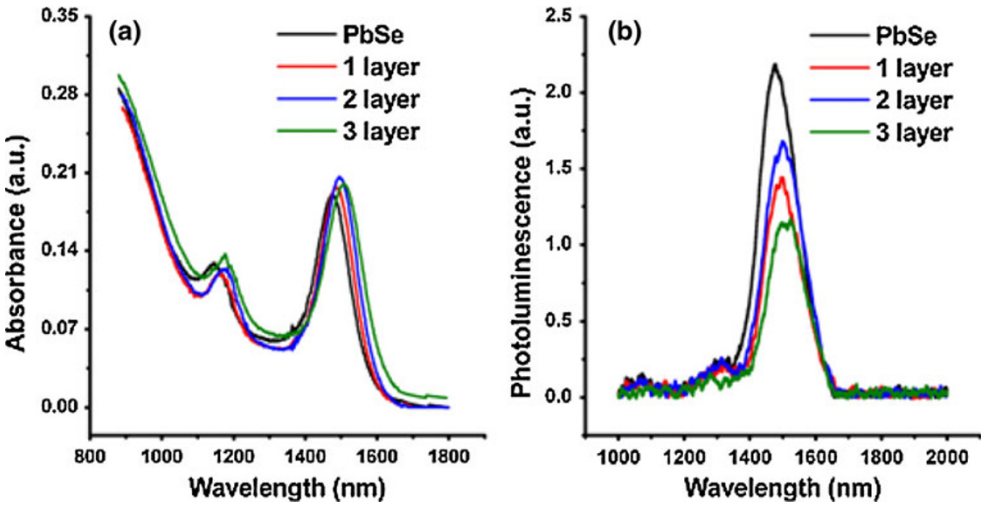

Fig. 2 Absorption (**a**) and photoluminescence (**b**) spectra recorded during CdSe shell growth. A consistent red shift of the peak wavelength (11, 10, 11 nm) was observed when one to three monolayers of CdSe shells grown on 4.8 nm PbSe cores

the thickness of energy barrier. Because the wavefunctions diffuse into shells, the confinement energy will change with the increase in shell thickness. According to Eq. 2,

$$\frac{dE^{conf}}{dR} = -\Delta t \frac{2E^{conf}}{R} \tag{7}$$

where Δt is the difference of transmission coefficients of electron and hole. From the energy levels shown in Fig. 3 [16–18], the expansion probability of electron is bigger than that of hole because of the lower barriers of electron according to the very closed effective masses of electron and hole ($m_e^* = 0.070$, $m_h^* = 0.068$). In this case, one nanometer shell barrier will result in a decrease in 17.55 meV for the confinement energy. We have also calculated that the increase in Coulomb energy is 0.068 meV for one nanometer barrier. Correspondingly, the red shifts of the first excitonic absorption peak for three individual monolayer CdSe shells are counted as 10.81, 9.45, and 8.36 nm, respectively. They are in good agreement for the experimental data taking account of the effect of surface polarization energy.

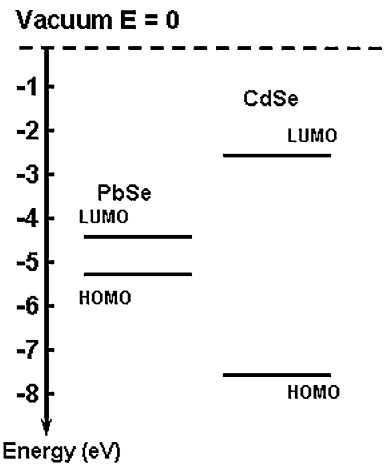

Fig. 3 LUMO and HOMO structures for 4.8 nm PbSe QDs and 0.35 nm CdSe shell

The third term in Eq. 1 is the surface-polarization energy that affects the gap energy E_{gap}, which is the Stark effect. A certain number of defect states are expected on the surface of unpassivated PbSe QDs. Therefore, charge carriers trapped on or near the surface of QDs may generate localized electric fields, where delocalized exciton states within the QDs can be highly polarizable. The surface polarization energy $\Delta E^{pol} = E_e^{pol} + E_h^{pol}$ versus local electric field ξ is given by [19]

$$\Delta E^{pol} = \mu\xi + \frac{1}{2}\alpha\xi^2 + \cdots. \tag{8}$$

where μ and α are the resolved exciton dipole and polarizability, respectively. According to Muller et al.'s work [20], the spectrum shift of CdSe nanorods depends on the direction of the external electric field. The positive electric field induces red shift, and the negative one leads to blue shift. Since the QDs in this work are spherical (zero dimensional), it is reasonable that their peak shifts are independent of the direction of the electric field. Both positive and negative electric field can cause the emission peak to red shift, and the red shift increases when the electric field is stronger [21].

It has been known that unpassivated PbSe QDs surface is a Pb atom-rich shell [6, 7]. Therefore, there may be polarization charges on the surface of PbSe QDs which generate surface-polarization energy. However, the polarization charges are neutralized, because Pb atoms on the surface of PbSe QDs connect to oleic acid (the organic ligand used in the synthesis). The quantum yield of fresh PbSe QDs was 85% using IR-26 as a reference. When the PbSe/CdSe core/shell was synthesized, CdSe contacted with Pb atoms instead of oleic acid; this induced the increase of surface polarization charges. The spectra shift to red because of the enhancement of the Stark effect (Fig. 2).

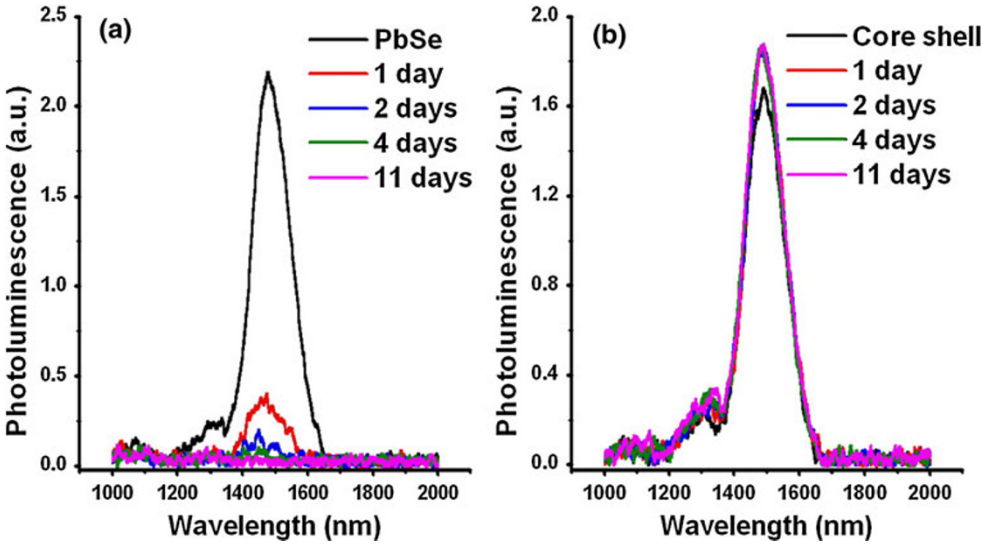

Fig. 4 The stability of PbSe (**a**) and PbSe/CdSe (**b**) QDs. The CdSe shells prevent PbSe core from the destructive oxidation. Compared with the unstable PbSe core, the PbSe/CdSe QDs remained unchanged

Different crystal lattices and thermal expansivities for PbSe and CdSe will more or less induce surface defects at the interface of the two materials [22]. The carriers will be trapped and result in the enhancement of the Stark effect. Such local fields cause the first exciton peak to shift to red and suppress the emission strength due to a reduced electron–hole wavefunction overlap. Unbalanced charges may also decrease the photoluminescence efficiency (quantum yield) via nonradiative Auger recombination.

The new traps were induced by surface defects depend on the shell growth. Compared with the photoluminescence of one monolayer core/shell QDs, the photoluminescence of two monolayers core/shell QDs increased as shown in Fig. 2b. However, it was found that more shell layers resulted in a decrease in photoluminescence strength (Fig. 2b). That is also because the tensile change at the interface is nonlinear with the shell thickness. When PbSe QDs were covered with two layers of CdSe, the good lattice tensility at the interface reduced the lattice mismatch and therefore increased the photoluminescence strength. When PbSe QDs were covered by three layers of CdSe, the lattice tensility was stronger and hence the photoluminescence strength decreased. Even so the quantum yield was still as high as 70% for our PbSe/CdSe core/shell QDs (IR-26 as the reference).

PbSe QDs are unstable even under the ambient conditions (room temperature and room light in air) (Fig. 4a). The destructive oxidation [6, 23] processes from the QDs surface inward. This process for each particle induces the effective particle size decrease and the blue shift of the spectrum. The particle collision in solution also contributes to the instable emission strength [6]. The oxidized surface can be peeled off after inelastic interparticle collisions. When the old oxidized surface is gone, the new surface will be oxidized quickly. For PbSe/CdSe core/shell structures, CdSe shells effectively prevent PbSe cores from the quick oxidation. The lifetime of PbSe QDs under ambient conditions therefore can be extended from a few days to at least a month (currently available data). The quantum yield remained the same in this period (Fig. 4b).

In conclusion, PbSe/CdSe core/shell QDs with a quantum yield of 70% were synthesized. The surface polarization and the expansion of carriers' wavefunctions contributed to the spectral red shift. The spectra red shifts during the formation of CdSe shells were calculated, and they exhibited a good fit to the experimental data. The stability of PbSe QDs was dramatically improved by the formation of CdSe shells.

Acknowledgments The funding supports from the State Key Laboratory on Integrated Optoelectronics, College of Electronic Science and Engineering, Jilin University, the Worcester Polytechnic Institute, and the National 863 Projects of China (2007AA03Z112, 2007AA06Z112) are acknowledged.

References

1. D. Cui, J. Xu, T. Zhu, G. Paradee, S. Ashok, M. Gerhold, Harvest of near infrared light in PbSe nanocrystal-polymer hybrid photovoltaic cells. Appl. Phys. Lett. **88**, 183111 (2006)
2. L. Levina, V. Sukhovatkin, S. Musikhin, S. Cauchi, R. Nisman, D.P. Bazett-Jones, E.H. Sargent, Efficient infrared-emitting PbS quantum dots grown DNA and stable in aqueous solution and blood plasma. Adv. Mater. **17**, 1854 (2005)
3. C.B. Murray, S. Sun, W. Gaschler, H. Doyle, T.A. Betley, C.R. Kagan, Colloidal synthesis of nanocrytals and nanocrystal superlattices. IBM J. Res. Dev. **45**, 47 (2001)

4. W.W. Yu, J.C. Falkner, B.S. Shih, V.L. Colvin, Preparation and characterization of monodisperse PbSe semiconductor nanocrystals in a noncoordinating solvent. Chem. Mater. **16**, 3318 (2004)
5. J.M. Pietryga, R.D. Schaller, D. Werder, M.H. Stewart, V.I. Klimov, J.A. Hollingsworth, Pushing the band gap envelope: mid-infrared emitting colloidal PbSe quantum dots. J. Am. Chem. Soc. **126**, 11752 (2004)
6. Q. Dai, Y. Wang, Y. Zhang, X. Li, R. Li, B. Zou, J. Seo, Y. Wang, M. Liu, W.W. Yu, Stability study of PbSe semiconductor nanocrystals over concentration, size, atmosphere, and light exposure. Langmuir **25**, 12320 (2009)
7. I. Moreels, B. Fritzinger, J.C. Martins, Z. Hens, Surface chemistry of colloidal PbSe nanocrystals. J. Am. Chem. Soc. **130**, 15081 (2008)
8. J. Xu, D. Cui, T. Zhu, G. Paradee, Z. Liang, Q. Wang, S. Xu, A.Y. Wang, Synthesis and surface modification of PbSe/PbS core-shell nanocrystals for potential device application. Nanotechnology **17**, 5428 (2006)
9. T.T. Tan, S.T. Selvan, L. Zhao, S. Gao, J.Y. Ying, Size control, shape evolution, and silica coating of near-infrared-emitting PbSe quantum dots. Chem. Mater. **29**, 3112 (2007)
10. J.M. Pietryga, D.J. Werder, D.J. Williams, J.L. Casson, R.D. Schaller, V.I. Klimov, J.A. Hollingsworth, Utilizing the lability of lead selenide to produce heterostructured nanocrystals with bright, stable infrared emission. J. Am. Chem. Soc. **130**, 4879 (2008)
11. J.J. Li, A.Y. Wang, W. Guo, J.C. Keay, T.D. Mishima, M.B. Johnson, X. Peng, Large-scale synthesis of nearly monodisperse CdSe/CdS core/shell nanocrystals using air-stable reagents via successive ion layer adsorption and reaction. J. Am. Chem. Soc. **125**, 12567 (2003)
12. Q. Dai, Y. Wang, X. Li, Y. Zhang, D.J. Pellegrino, M. Zhao, B. Zou, J. Seo, Y. Wang, W.W. Yu, Size-dependent composition and molar extinction coefficient of PbSe semiconductor nanocrystals. ACS Nano. **3**, 1518 (2009)
13. J.M. An, A. Franceschetti, A. Zunger, Electron and hole addition energies in PbSe quantum dots. Phys. Rev. B. **76**, 045401 (2007)
14. A. Olkhovets, R.-C. Hsu, A. Lipovskii, F.W. Wise, Size-dependent temperature variation of the energy gap in lead-salt quantum dots. Phys. Rev. Lett. **81**, 3539 (1998)
15. A.C. Phillips, *Introduction to Quantum Mechanics* (John Wiley & Sons Ltd., West Sussex, England, 2003), pp. 94–99
16. B. Hyun, Y. Zhong, A.C. Bartnik, L. Sun, H.D. Abruña, F.W. Wise, J.D. Goodreau, J.R. Matthews, T.M. Leslie, N.F. Borrelli, Electron injection from colloidal PbS quantum dots into titanium dioxide nanoparticles. ACS Nano. **2**, 2206 (2008)
17. C. Querner, P. Reiss, J. Bleuse, A. Pron, Chelating ligands for nanocrystals' surface fuctionalization. J. Am. Chem. Soc. **126**, 11574 (2004)
18. W.W. Yu, L. Qu, W. Guo, X. Peng, Experimental determination of the extinction coefficient of CdTe, CdSe, and CdS nanocrystals. Chem. Mater. **15**, 2854 (2003)
19. S.A. Empedocles, M.G. Bawendi, Quantum-confined stark effect in single CdSe nanocrystallite quantum dots. Science **278**, 2114 (1997)
20. J. Muller, J.M. Lupton, P.G. Lagoudakis, F. Schindler, R. Koeppe, A.L. Rogach, J. Feldmann, D.V. Talapin, H. Weller, Wave function engineering in elongated semiconductor nanocrystals with heterogeneous carrier confinement. Nano Lett. **5**, 2044 (2005)
21. L. Qian, D. Bera, T. Tseng, P.H. Holloway, High efficiency photoluminescence from silica-coated CdSe quantum dots. Appl. Phys. Lett. **94**, 073112 (2009)
22. B.H. Koo, T. Hanada, H. Makino, T. Yao, Effect of lattice mismatch on surface morphology of in as quantum dots on (100) $In_{1-x}Al_xAs/InP$. Appl. Phys. Lett. **79**, 4331 (2001)
23. J.W. Stouwdam, J. Shan, F.C.J.M. van VeggelAndras, A.G. Pattantyus-Abraham, J.F. Young, Photostability of colloidal PbSe and PbSe/PbS core/shell nanocrystals in solution and in the solid state. J. Phys. Chem. C. **111**, 1086 (2007)